

Phase-sensitive nonclassical properties in quantum metrology with displaced squeezed vacuum state

ZHIWEI TAO^{1,2}, YICHONG REN^{2,*}, AZEZIGUL ABDUKIRIM², SHIWEI LIU^{1,2}, AND RUIZHONG RAO²

¹School of Environmental Science and Optoelectronic Technology, University of Science and Technology of China, Hefei 230022, China

²Key Laboratory of Atmospheric Optics, Anhui Institute of Optics and Fine Mechanics, Chinese Academy of Sciences, Hefei 230031, China

*Corresponding author: rych@aiofm.ac.cn

Compiled May 4, 2021

We predict that the phase-dependent error distribution of locally unentangled quantum states directly affects quantum parameter estimation accuracy. Therefore, we employ the displaced squeezed vacuum (DSV) state as a probe state and investigate an interesting question of the phase-sensitive nonclassical properties in DSV's metrology. We found that the accuracy limit of parameter estimation is a function of the phase-sensitive parameter $\phi - \theta/2$ with a period π . We show that when $\phi - \theta/2 \in [k\pi/2, 3k\pi/4]$ ($k \in \mathbb{Z}$), we can obtain the accuracy of parameter estimation approaching the ultimate quantum limit through using the DSV state with the larger displacement and squeezing strength, whereas $\phi - \theta/2 \in (3k\pi/4, k\pi]$ ($k \in \mathbb{Z}$), the optimal estimation accuracy can be acquired only when the DSV state degenerates to squeezed-vacuum state. © 2021 Optical Society of America

<http://dx.doi.org/10.1364/JOSAB.XX.XXXXXX>

1. INTRODUCTION

Quantum metrology, also known as quantum parameter estimation, primarily focuses on enhancing the measurement accuracy of parameter estimation in the dynamical evolution of the quantum probe system by using the features of quantum mechanics, which demonstrates an impressive significance both in theoretical predictions and experiments[1–4]. At the early stage, the improvement sought is an enhanced sensitivity achieved by a given number of resources, such as number of probes, mean and maximum energy, number of measurements and choice of integration time. However, without any quantum instruments, the actual accuracy limit that can be achieved is determined by the quantum noise of a single photon after quantization of the electromagnetic field, in quantum optics typically so-called the shot-noise limit[5].

On the other hand, the optimal estimation accuracy is also bound by the uncertainty principle of quantum mechanics, which easily translates into $1/N$ scaling of Heisenberg limit[5] on parameter estimation using an N -photon state. To beat the shot-noise limit and constantly approach the Heisenberg scaling, most commonly alternative quantum features such as entanglement[4, 6–11], correlations[12, 13], non-trivial Hamiltonians[14–16] and identical particles[17, 18] have been employed to improve measurement accuracy over past decades substantially. Especially, many researchers have focused their efforts primarily on how to find the optimal probe state and measurement for estimating any parameter or multiple parameters encoded in a bosonic Gaussian channel[5, 19–28] and achieve

exactly the same estimation precision as entangled probes.

However, although they have elaborated general methods for improving the parameter estimation accuracy extensively, very little research has been conducted on another important physical issue: Where the parameter estimation error arises? Notably, it is well-known that the role of the unitary parameter operator makes the input state obtain a fixed parameter shift. Therefore, we now have to pose the theoretically important question: why does the estimated parameter have a standard deviation? We intuitively believe that for unentangled local quantum states, the error that comes from the estimated parameters might be partially determined by the initial phase distribution of the input quantum state. In other words, the error contour's shape of the input quantum state[29] might directly affect the parameter estimation accuracy. Additionally, since quantum Fisher information (QFI) is associated with the distinguishability of two infinitely close-by quantum states[21], we anticipate that both combinations might jointly impact the accuracy limit of parameter estimation.

To examine our anticipation, in this work, we employ the displaced squeezed vacuum (DSV) state as a probe state and investigate their phase-sensitive nonclassical properties in quantum metrology. DSV state, as a special form of single-mode Gaussian state, have several useful characteristics for our exploration such as it contains the phase-dependent noise, reduced below that of the coherent state for some phases and enhanced above that of the coherent state for others[30]. Because of this phase-dependent error distribution DSV state leads many technological

applications, particularly in the detection of weak signals[31–33]. Besides, in analogy to quadrature squeezing, another form of squeezing such as number squeezing can also be accomplished by rotating the DSV's phase $\phi - \theta/2$ coming from the squeezing parameter $\xi = re^{i\theta}$ and displacement parameter $\alpha = |\alpha| e^{i\phi}$ [30], as depicted in Fig. 1.

Based on the above nonclassical properties, we first evaluate whether the compound phase-sensitive parameter $\phi - \theta/2$ is connected to the Cramer-Rao limit of the DSV state and then give a quantitative relationship between $\phi - \theta/2$ and the QFI of the single-mode DSV state. Our conclusion is that the accuracy limit of parameter estimation is a periodic function of $\phi - \theta/2$ with a period π , which is influenced by, but not uniquely influencing, the compound physical quantity. When $\phi - \theta/2 \in [k\pi/2, 3k\pi/4]$ ($k \in \mathbb{Z}$), the DSV state with the larger squeezing strength and displacement can achieve the most accurate parameter estimation performance, whereas in the $\phi - \theta/2 \in (3k\pi/4, k\pi]$ ($k \in \mathbb{Z}$) regime, the same effect can be obtained only when the DSV state degenerates to a squeezed-vacuum state.

The paper is structured as follows. In Sec. 2, we briefly introduce the concept of QFI and define the phase-sensitive parameter $\phi - \theta/2$, notably, $\phi - \theta/2$ keep invariance under the parameterization process. In Sec. 3, to rule out the overestimation of parameter information[34–37], we first calculate the QFI of the single-mode DSV state after introducing an external parameter reference. Secondly, based on the results of the DSV's QFI, we investigate how the accuracy limit of parameter estimation changes with respect to the phase-sensitive parameter under some typical displacement and squeezing parameters. Then, we analyze a more general result about how these intrinsic DSV's parameters interplay the accuracy limit of parameter estimation under different phase-sensitive conditions and find what pair of DSV's intrinsic parameters gives the optimal estimation accuracy under some typical phase-sensitive conditions. Our main results are summarized in Sec. 4.

2. THEORY

A. Quantum Fisher information

Generally speaking, the procedure of parameter estimation can be roughly decomposed into four steps: probe state preparation, parameterization or dynamical evolution, measurement of the parameter encoded state as well as estimation of parameter through postprocessing the measurement data. Thus, from the above four steps, it is clearly shown to us that there exists an optimal measurement strategy allowing the parameter estimation with the highest accuracy. Assuming that the parameter to be estimated is one of the variables φ in the system, then the estimated limit is followed by quantum Cramer-Rao inequality[38, 39]

$$\Delta^2 \varphi \geq \frac{1}{MI_\varphi} \quad (1)$$

where M is the number of measurements in experiments, I_φ stands for QFI associated with the measurement accuracy and $\Delta^2 \varphi$ represents the variance of the parameter φ .

QFI is a natural generalization of the variance of the classical score function, which measures the amount of information contained in a parameterized random variable, defined as follows

$$I_\varphi = \text{Tr} \left(\rho_\varphi L_{\rho_\varphi}^2 \right) \quad (2)$$

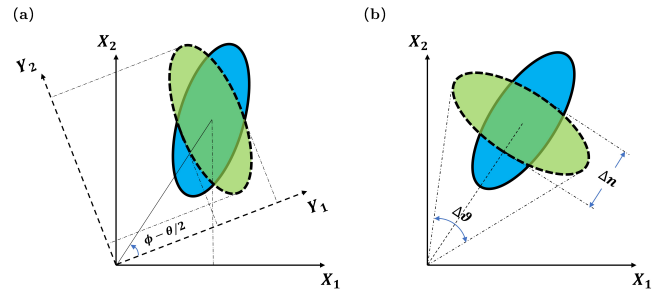


Fig. 1. Error ellipse in complex amplitude plane for the DSV state $D(\alpha)S(\xi)|0\rangle$, where $\xi = re^{i\theta}$ and $\alpha = |\alpha| e^{i\phi}$. (a) Definition of phase-sensitive parameter $\phi - \theta/2$; (b) Rotated error ellipse with $\phi - \theta/2 = k\pi/2$ ($k \in \mathbb{Z}$) and $\phi - \theta/2 = k\pi$ ($k \in \mathbb{Z}$), where $\Delta\theta$ and Δn represent the phase uncertainty and the amplitude uncertainty for given rotation angle respectively.

where ρ_φ is the probe state after parametrical encoding, L_{ρ_φ} is the symmetric logarithmic derivative determined by $\partial_\varphi \rho_\varphi = 1/2 (L_{\rho_\varphi} \rho_\varphi + \rho_\varphi L_{\rho_\varphi})$. Another physical meaning of QFI is that it geometrically measures the distinguishability between two quantum states $\rho(\varphi)$ and $\rho(\varphi + d\varphi)$ that differ infinitesimally in $d\varphi$, which can also be expressed by the Bures distance[40]

$$I_\varphi = 4ds_{\text{Bures}}^2(\rho(\varphi), \rho(\varphi + d\varphi)) / d\varphi^2 \quad (3)$$

where $ds_{\text{Bures}}^2(\rho, \sigma) \equiv 2 \left[1 - \sqrt{F(\rho, \sigma)} \right]$ denotes the Bures distance and $F(\rho, \sigma) \equiv \left[\text{Tr}(\sqrt{\sqrt{\rho}\sigma\sqrt{\rho}}) \right]^2$ is the Uhlmann fidelity.

For pure states $\rho_\varphi = |\psi_\varphi\rangle\langle\psi_\varphi|$, the QFI simplifies to the overlap of the derivative of the state with itself and the original state, which can be described as[5]

$$I_\varphi = 4 \left(\langle \partial_\varphi \psi_\varphi | \partial_\varphi \psi_\varphi \rangle + |\langle \partial_\varphi \psi_\varphi | \psi_\varphi \rangle|^2 \right) \quad (4)$$

where $|\partial_\varphi \psi_\varphi\rangle = \partial |\psi_\varphi\rangle / \partial \varphi$. Generally, parameterization for a given scenario is not always straightforward and can lead to different results[34]. Therefore, to prevent the exaggerated estimation of QFI, an external parameter reference is invoked to allow a well-defined parameter φ . In the absence of parameter reference, one has to pay attention to what parameter encoding strategies are required to the corresponding experimental setup for attaining the accurate QFI[41–43].

Therefore, if we consider the input state $|\psi\rangle$ of two modes, the above procedure becomes a two-parameter estimation problem and a QFI matrix needs to be employed. Assuming the two parameters introduced is φ_1 and φ_2 , under the basis $\varphi_\pm = \varphi_1 \pm \varphi_2$, the process of parametrical encoding can be realized by[36]

$$|\psi_\varphi\rangle = \exp[i(\varphi_+ G_+ + \varphi_- G_-)] |\psi\rangle \quad (5)$$

where $G_+ = \frac{1}{2}(\hat{a}^\dagger \hat{a} + \hat{b}^\dagger \hat{b})$ and $G_- = \frac{1}{2}(\hat{a}^\dagger \hat{a} - \hat{b}^\dagger \hat{b})$. \hat{a} , \hat{b} denotes photon annihilation operators for the signal and the idler. Since we are interested in the variance of φ_- , the element of QFI matrix I_{--} can be calculated following Eq. (4) by[44]

$$I_{--} = 4\text{Var}(G_-) = 4 \left(\langle \psi_\varphi | G_-^2 | \psi_\varphi \rangle - |\langle \psi_\varphi | G_- | \psi_\varphi \rangle|^2 \right) \quad (6)$$

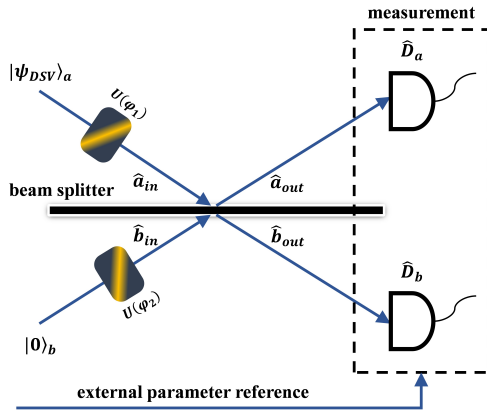


Fig. 2. Interferometric parameter estimation scheme for the DSV state. The difference between $\varphi_1 - \varphi_2$ is estimated, based on the measurement strategies \hat{D}_a and \hat{D}_b . The external parameter estimation is employed to prevent the overestimation of the DSV's QFI.

B. Phase-sensitive parameter of the DSV state

A coherent state has half of unity identical uncertainty both in the horizontal and vertical direction, which is the closest quantum state to the classical one. Hence, to reduce the noise in one of two directions, the common strategy can be realized by squeezing the wave packet at the expense of the corresponding increased fluctuations in the conjugate direction. Theoretically, the squeezed state can be usually generated by the secondary action of the squeeze operator $S(\xi)$ and the displacement operator $D(\alpha)$ on the vacuum state

$$|\psi\rangle \equiv S(\xi) D(\alpha) |0\rangle \quad (7)$$

where $\xi = re^{i\theta}$ and $\alpha = |\alpha|e^{i\phi}$. θ and ϕ constitute the phase-sensitive parameter shown in Fig. 1(a). Another definition called the DSV state is considered in this paper through exchanging the two unitary transformations imprinted on the vacuum state. Notably, these two operators do not commute with each other, which connect by the following relationship[30, 45]

$$\begin{aligned} S(\xi) D(\alpha) &= D(\beta) S(\xi) \\ \beta &= \alpha \cosh r + \alpha^* e^{i\theta} \sinh r \end{aligned} \quad (8)$$

As shown in Fig. 1(b), we observe the rotation of the DSV's error contour leads to different uncertainties both in the phase and amplitude of electric field (e.g., the green ellipse with dashed line has a maximum phase uncertainty $\Delta\theta$ and minimum amplitude uncertainty Δn , nevertheless, the situation is reversed for the error contour counterclockwise rotating $\pi/2$, see the blue one with full line). With this in mind, we somewhat intuitively considered that selecting an appropriate squeeze direction such as a decreased phase uncertainty may facilitate us to obtain more accurate information about the unknown parameters. Concretely, when the compound physical quantity $\phi - \theta/2$ (illustrate in Fig. 1(a)), we called a phase-sensitive parameter, equals to an integer multiple of $\pi/2$, the DSV state may achieve better performance for parameter estimation compared with coherent states. Conversely, the reversed conclusions may be acquired when $\phi - \theta/2 = k\pi$ ($k \in \mathbb{Z}$).

3. RESULTS

A standard Mach-Zehnder interferometer with two arms a and b usually consists of two 50 : 50 beam splitters and a phase shifter. The input photons passing through the first beam splitter introduce a parameter to be estimated. Then, these two photons interfere at the second beam splitter. Finally, the magnitude of the parameter can be estimated from measurement outcomes through data postprocessing. An important reason why such a scheme effectively improves the accuracy of parameter estimation is that the first beam splitter converts the incident photonic state into a path-entangled state, thus enabling quantum-enhanced measurements.

In the present contribution, we consider an interferometer without including the first beam splitter for achieving the same performance compared with entanglement, the initial DSV state and the vacuum state prepared in mode a and b , as shown in Fig. 2, and acquired two phase shifts φ_1 and φ_2 in the channel a and b respectively. Undergoing the parametrical encoding, the QFI of the output state $|\psi_\varphi\rangle$ in Eq. (6) can be expressed by

$$\begin{aligned} I_{--} &= \sinh^2 r \cosh^2 r - |\alpha|^2 \{2 \sinh r \cosh r \cos [2(\phi - \theta/2)] - 1\} \\ &+ (2|\alpha|^2 + 1) \sinh^2 r + \sinh^4 r \end{aligned} \quad (9)$$

Substituting the above equation into Eq. (1), we can achieve the Cramer-Rao limit for the DSV state. It can be seen from the above equation that the maximum accuracy of parameter estimation is a function of $\phi - \theta/2$ with a period of π . when $\phi - \theta/2 = k\pi$ ($k \in \mathbb{Z}$), since I_{--} obtains the minimum values, the worst accuracy will be acquired at this moment. On the contrary, the reversed conclusions are reported under a better phase-sensitive circumstance, which is the same as our previous conjecture.

Before the formal discussion, we state that the above-mentioned Heisenberg limit is commonly defined as the inverse of the average photon number \bar{n} of the input state (i.e., $\Delta\varphi_{HL} = 1/\bar{n}$). However, it should be noted that the ultimate accuracy of parameter estimation will be underestimated if the photon number fluctuations are neglected, especially in the high fluctuations regime. Therefore, to prevent this underestimation, a more direct definition of the ultimate quantum limit in Hofmann[46] typically for scaling as $1/\sqrt{\bar{n}^2}$ with averaged squared photon numbers \bar{n}^2

$$\begin{aligned} \bar{n}^2 &= |\alpha|^4 - |\alpha|^2 \{2 \sinh r \cosh r \cos [2(\phi - \theta/2)] - 1\} \\ &+ \sinh^2 r \cosh^2 r + (4|\alpha|^2 + 1) \sinh^2 r \\ &+ 2 \sinh^4 r \end{aligned} \quad (10)$$

A. Under the same phase-sensitive condition

The comparison of the Cramer-Rao, the Hofmann, and the shot-noise limit as a function of $\phi - \theta/2$ is presented in Fig. 3 for different typical squeezing strengths and displacements. As shown in the top row of Fig. 3, we observe that in the $\phi - \theta/2 = k\pi/2$ ($k \in \mathbb{Z}$) regime, the Cramer-Rao limit of the DSV state beats the $1/\sqrt{\bar{n}}$ scaling of shot-noise limit. Under the same squeezing strength and displacement, it is not strange that the accuracy limit of parameter estimation is overall inferior that the shot-noise limit when $\phi - \theta/2 = k\pi$ ($k \in \mathbb{Z}$), notably, such

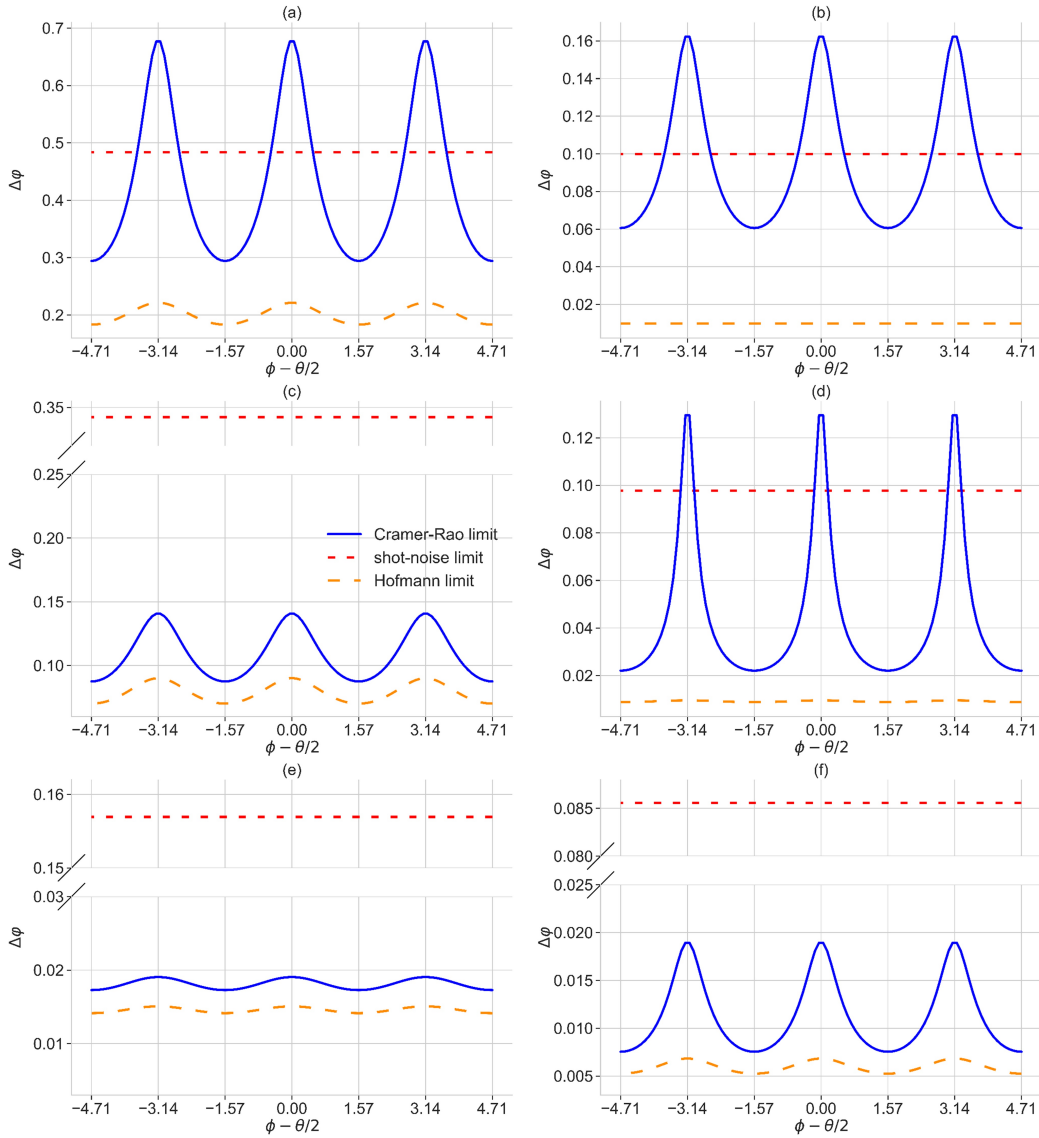


Fig. 3. Accuracy limit of parameter estimation as a function of the compound phase-sensitive parameter $\phi - \theta/2$ in the range $[-3\pi/2, 3\pi/2]$ for different displacements and squeezing strengths (a) $r = 0.5$, $|\alpha| = 2$ (b) $r = 0.5$, $|\alpha| = 10$ (c) $r = 1.5$, $|\alpha| = 2$ (d) $r = 1.5$, $|\alpha| = 10$ (e) $r = 2.5$, $|\alpha| = 2$ (f) $r = 2.5$, $|\alpha| = 10$.

conclusions presented both in Fig. 3(a) and 3(b) are consistent with our intuitive prediction.

Meanwhile, we also explore the larger squeezing strength $r = 1.5$ under the same displacement in Fig. 3(c). It is clearly found that the accuracy limit of parameter estimation in the situation of $\phi - \theta/2 = k\pi/2$ ($k \in \mathbb{Z}$) will not only break the shot-noise limit but also approach the Hofmann scaling, even when the phase sensitivity condition is not favorable ($\phi - \theta/2 = k\pi$ ($k \in \mathbb{Z}$)), the accuracy limit can likewise beat the shot-noise limit, which may somewhat counterintuitively. The possibility arises because QFI describes how rapidly quantum fidelity changes between two infinitesimally different states. When the squeezing strength becomes larger, although the error ellipse radius of the DSV state surpasses coherent state under a bad phase-sensitive condition, QFI is more sensitive to the parameter, infinitesimal changes may lead the QFI rapidly changed after parametrical encoding, the combination of which results in the estimated accuracy limit has superior sensitivity compared with the shot-noise limit. The

conclusions constituted through adjusting $r = 1.5$, $|\alpha| = 10$ in Fig. 3(d) are the same as what we achieve in Fig. 3(b).

Moreover, with the squeezing strength increased to $r = 2.5$ (illustrate in Fig. 3(e) and 3(f)), a smaller displacement may enable the DSV state to lose its phase-sensitive advantages. At this moment, the accuracy limit of parameter estimation has a better approach to the Hofmann limit regardless of its phase-sensitive characteristics. Comparing the magnitudes of the different displacement $|\alpha|$ of the DSV states, the state with the largest $|\alpha|$ performs the best on the estimation because of its the largest error contour angle $\Delta\theta$.

B. Under the same average photon number

We illustrate in Fig. 4 how the Cramer-Rao lower bound changes with respect to the average photon number \bar{n} for any possible squeezing strength and displacement. The different spacing dashed lines represent the DSV state with the equal r but \bar{n} varying, which indicates that increasing the DSV's squeezing

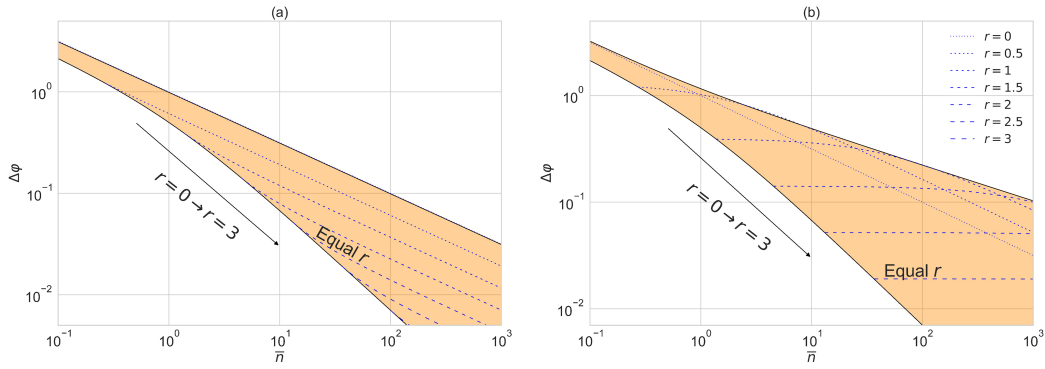


Fig. 4. Accuracy limit of parameter estimation as a function of the average photon number \bar{n} for any $|\alpha|$ and r under different typical phase-sensitive conditions (a) $\phi - \theta/2 = \pi/2$ (b) $\phi - \theta/2 = 0$. The shaded region represents all possible estimation error for any combination of $|\alpha|$ and r . The different spacing dashed lines represent the DSV state with the equal r but \bar{n} varying.

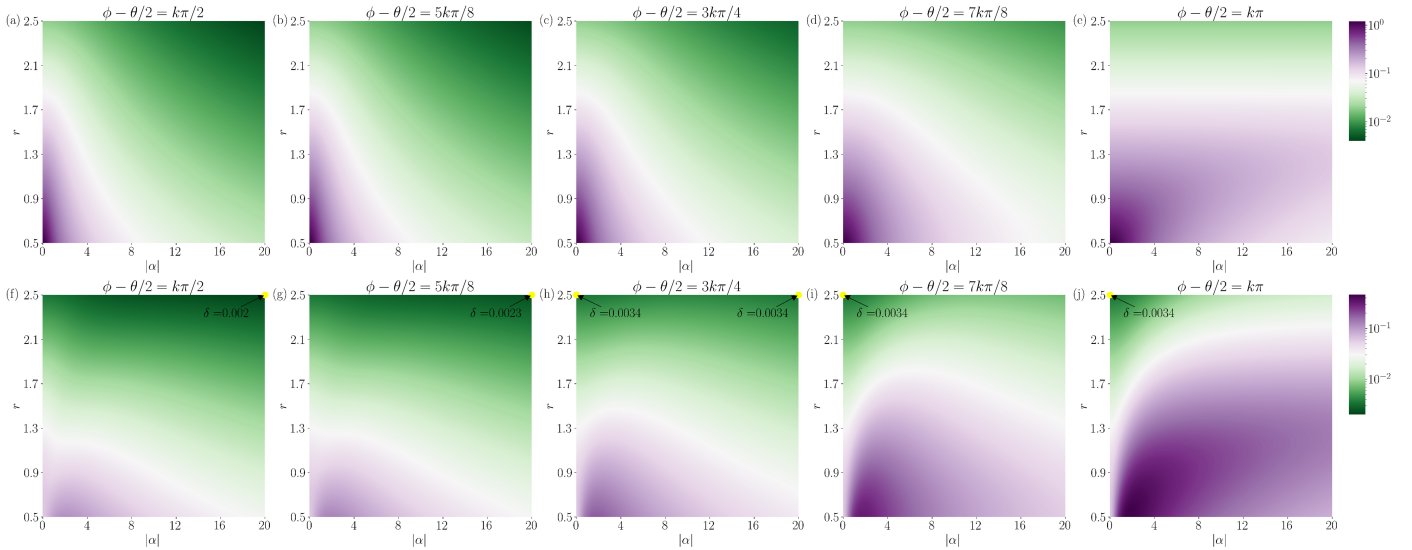


Fig. 5. The density plots represent the accuracy limit of parameter estimation ((a)–(e)) and the difference between the accuracy limit and the Hofmann limit ($\delta \equiv \Delta\phi - \Delta\phi_{Hof}$) ((f)–(j)) as a function of $|\alpha|$ and r under different phase-sensitive conditions (a), (f) $\phi - \theta/2 = k\pi/2$ ($k \in \mathbb{Z}$); (b), (g) $\phi - \theta/2 = 5k\pi/8$ ($k \in \mathbb{Z}$); (c), (h) $\phi - \theta/2 = 3k\pi/4$ ($k \in \mathbb{Z}$); (d), (i) $\phi - \theta/2 = 7k\pi/8$ ($k \in \mathbb{Z}$); (e), (j) $\phi - \theta/2 = k\pi$ ($k \in \mathbb{Z}$). Optimal points which have the most approach to the Hofmann limit have been labeled in each plot by solid yellow dots. The colorbar for all density plots in each row are the same.

strength can constantly improve the accuracy limit of parameter estimation. The upper boundary of the shaded area in Fig. 4(a) stands for the shot-noise limit, corresponding to the shortest spacing dashed line in Fig. 4(b). In the $\phi - \theta/2 = \pi/2$ regime, (Fig. 4(a)), representing the phase-sensitive condition of any integer multiple of $\pi/2$, the DSV state with the larger squeezing strength achieves the higher parameter estimation accuracy as \bar{n} increases, which coincides with our qualitatively geometric intuitive prediction.

Moreover, as compared with the results acquired in the favorable phase-sensitive condition, we find in Fig. 4(b) (i.e., in the $\phi - \theta/2 = 0$ regime, representing the phase-sensitive condition of any integer multiple of π) that the accuracy limit of parameter estimation is the same as the circumstance presented in Fig. 4(a) when the DSV state with no displacement. However, this superiority of the squeezed-vacuum state gradually decreases as $|\alpha|$ increases. Notably, we observe that for the DSV state with different squeezing strengths, the Cramer-Rao lower bound hardly

varies with \bar{n} and still beats the shot-noise limit within a specific photon number range (e.g., when $r = 1.5$, the DSV state with $\bar{n} \in (0, 55]$ yields superior performance than the shot-noise limit, which is not shown in Fig. 4). When $|\alpha|$ increases until the accuracy limit of parameter estimation exceeds the shot-noise limit, parameter estimation employing the DSV state under this phase-sensitive condition may obtain much less effective than that of the coherent state.

C. Under the same squeezing strength and displacement

In order to give a general analysis about how displacement and squeezing parameter interplay the accuracy limit of parameter estimation and find what a pair of displacement and squeezing parameter gives the optimal parameter estimation accuracy, we present the density plot of $\Delta\phi$ as a function of $|\alpha|$ and r in the top row of Fig. 5, manifesting the Cramer-Rao limit monotonically decreases as $|\alpha|$ and r increase. Besides, we employ the Hofmann limit as a benchmark to measure the optimality of intrinsic DSV's parameters. The bottom row of Fig. 5 presents the difference

density plot between the Cramer-Rao limit and the Hofmann limit under some typical phase-sensitive conditions.

Based on the comparison of five plots in the top row of Fig. 5, we conclude the results from the parameter estimation error evolution: the DSV state with the larger squeezing strength and displacement may achieve a lower estimation error of parameter except Fig. 5(e) (i.e., in the $\phi - \theta/2 = k\pi$ ($k \in \mathbb{Z}$) regime). We observe in Fig. 5(e) that when r beyond a certain range, the increase of $|\alpha|$ might not enhance the parameter estimation performance (e.g., $r = 2$). Besides, we also find that when $|\alpha|$ is fixed and surpasses the specific threshold, the DSV state with the larger r might not obtain a higher estimation accuracy (e.g., $|\alpha| = 10$). These possibilities can be geometrically explained by the compromise of the smaller error ellipse radius and larger fidelity susceptibility [47, 48] discussed in Fig. 3(c).

The optimal measurement accuracy of parameter estimation is marked at each density plot in the bottom row of Fig. 5 with solid yellow dots. As depicted in Fig. 5(h) to (j), we indicate that the DSV's optimal estimation accuracy is obtained at the left upper corner, where $|\alpha| = 0$. Especially, the right upper corner of Fig. 5(h) is also the optimal point that most approaching the Hofmann limit, which coincides with the conclusions discussed in Ref. [49]. Nevertheless, we observe in Fig. 5(f) and (g) that the optimality of intrinsic DSV's parameters will be transfer to the right upper corner of the density plot when $\phi - \theta/2 \in [k\pi/2, 3k\pi/4]$ ($k \in \mathbb{Z}$), which means that the DSV state with a better phase-sensitive characteristic and larger squeezing strength and displacement can significantly enhance the parameter estimation accuracy to the ultimate quantum limit.

4. CONCLUSIONS

In this paper, we first qualitatively assess the performance of parameter estimation under different phase-sensitive conditions from the perspective of a general quantum state's geometric error ellipse. Secondly, we explore the phase-sensitive nonclassical properties in quantum metrology using a single-mode DSV state. Similar to our geometric intuitive prediction, we found that the accuracy limit of DSV's parameter estimation is a function of the phase-sensitive parameter $\phi - \theta/2$ with period π . Besides, we also demonstrate that in the $\phi - \theta/2 = k\pi/2$ ($k \in \mathbb{Z}$) regime, the DSV state with the larger displacement $|\alpha|$ and squeezing strength r can significantly reduce the estimation error, whereas when $\phi - \theta/2 = k\pi$ ($k \in \mathbb{Z}$), the DSV state with equal $|\alpha|$ and larger r or equal r and larger $|\alpha|$ do not necessarily enhance the parameter estimation performance. We then demonstrate that under this circumstance, the selection of the smaller $|\alpha|$ combined with larger r can beat the shot-noise limit within a certain average photon number range.

Our initial aim is to reveal how the accuracy limit of parameter estimation changes with the DSV's phase-sensitive parameter and find what pair of DSV's intrinsic parameters gives the optimal parameter estimation accuracy under some typical phase-sensitive conditions. We indicate that the DSV state with the larger r and $|\alpha|$ can obtain the parameter estimation accuracy that is closest to the ultimate quantum limit when $\phi - \theta/2 \in [k\pi/2, 3k\pi/4]$ ($k \in \mathbb{Z}$), whereas $\phi - \theta/2 \in (3k\pi/4, k\pi]$ ($k \in \mathbb{Z}$), the same effect can be obtained only when the DSV state degenerates to a squeezed-vacuum state.

Funding. Anhui Provincial Natural Science Foundation (Grant

No. 1908085QA37); National Natural Science Foundation of China (Grant No. 11904369); State Key Laboratory of Pulsed Power Laser Technology Supported by Open Research Fund of State Key Laboratory of Pulsed Power Laser Technology (Grant No. 2019ZR07).

Acknowledgment. We thank the anonymous referee whose comments significantly improved the presentation of this paper.

Disclosures. The authors declare no conflicts of interest.

REFERENCES

1. V. Giovannetti, S. Lloyd, and L. Maccone, "Advances in quantum metrology," *Nat. Photon.* 5, 222 (2011).
2. M. A. Taylor and W. P. Bowen, "Quantum metrology and its application in biology," *Phys. Rep.* 615, 1 (2016).
3. C. L. Degen, F. Reinhard, and P. Cappellaro, "Quantum sensing," *Rev. Mod. Phys.* 89, 035002 (2017).
4. V. Giovannetti, S. Lloyd, and L. Maccone, "Quantum-enhanced measurements: beating the standard quantum limit," *Science* 306, 1330 (2004).
5. D. Braun, G. Adesso, F. Benatti, R. Floreanini, U. Marzolino, M. W. Mitchell, and S. Pirandola, "Quantum-enhanced measurements without entanglement," *Rev. Mod. Phys.* 90, 035006 (2018).
6. J. Joo, W. J. Munro, and T. P. Spiller, "Quantum metrology with entangled coherent states," *Phys. Rev. Lett.* 107, 083601 (2011).
7. Y. M. Zhang, X. W. Li, W. Yang, and G. R. Jin, "Quantum Fisher information of entangled coherent states in the presence of photon loss," *Phys. Rev. A* 88, 043832 (2013).
8. K. Berrada, S. A. Khalek, and C. H. Raymond Ooi, "Quantum metrology with entangled spin-coherent states of two modes," *Phys. Rev. A* 86, 033823 (2012).
9. J. Joo, K. Park, H. Jeong, W. J. Munro, K. Nemoto, and T. P. Spiller, "Quantum metrology for nonlinear phase shifts with entangled coherent states," *Phys. Rev. A* 86, 043828 (2012).
10. L. Zhang and K. W. C. Chan, "Quantum multiparameter estimation with generalized balanced multimode NOON-like states," *Phys. Rev. A* 95, 032321 (2017).
11. S. Y. Lee, C. W. Lee, J. Lee, and H. Nha, "Quantum phase estimation using path-symmetric entangled states," *Sci. Rep.* 6, 30306 (2016).
12. K. Modi, H. Cable, M. Williamson, and V. Vedral, "Quantum correlations in mixed-state metrology," *Phys. Rev. X* 1, 021022 (2011).
13. Y. Yao, X. Xiao, L. Ge, X. G. Wang, and C. P. Sun, "Quantum Fisher information in noninertial frames," *Phys. Rev. A* 89, 042336 (2014).
14. T. Tilma, S. Hamaji, W. J. Munro, and K. Nemoto, "Entanglement is not a critical resource for quantum metrology," *Phys. Rev. A* 81, 022108 (2010).
15. J. Beltran and A. Luis, "Breaking the Heisenberg limit with inefficient detectors," *Phys. Rev. A* 72, 045801 (2005).
16. M. J. Woolley, G. J. Milburn, and C. M. Caves, "Nonlinear quantum metrology using coupled nanomechanical resonators," *New J. Phys.* 10, 125018 (2008).
17. F. Benatti and D. Braun, "Sub-shot-noise sensitivities without entanglement," *Phys. Rev. A* 87, 012340 (2013).
18. M. Oszmaniec, R. Augusiak, C. Gogolin, J. Kołodyński, A. Acin, and M. Lewenstein, "Random bosonic states for robust quantum metrology," *Phys. Rev. X* 6, 041044 (2016).
19. D. Šafránek and I. Fuentes, "Optimal probe states for the estimation of Gaussian unitary channels," *Phys. Rev. A* 94, 062313 (2016).
20. A. Monras, "Optimal phase measurements with pure Gaussian states," *Phys. Rev. A* 73, 033821 (2006).
21. O. Pinel, P. Jian, N. Treps, C. Fabre, and D. Braun, "Quantum parameter estimation using general single-mode Gaussian states," *Phys. Rev. A* 88, 040102(R) (2013).
22. C. Oh, C. Lee, C. Rockstuhl, H. Jeong, J. Kim, H. Nha, and S. Y. Lee,

- "Optimal Gaussian measurements for phase estimation in single-mode Gaussian metrology," *npj Quantum Info.* 5, 10 (2019).
23. D. Šafránek, A. R. Lee, and I. Fuentes, "Quantum parameter estimation using multi-mode Gaussian states," *New J. Phys.* 17, 073016 (2015).
 24. R. Nichols, P. Liuzzo-Scorpo, P. A. Knott, and G. Adesso, "Multiparameter Gaussian quantum metrology," *Phys. Rev. A* 98, 012114 (2018).
 25. D. Šafránek, "Estimation of Gaussian quantum states," *J. Phys. A: Math. Theor.* 52, 035304 (2019).
 26. L. Bakmou, M. Daoud, and R. laamara, "Multiparameter quantum estimation theory in quantum Gaussian states," *J. Phys. A: Math. Theor.* 53, 385301 (2020).
 27. J. Zhang, "Quantum Fisher information for states in exponential form," *Phys. Rev. A* 89, 032128 (2014).
 28. N. Friis, M. Skotiniotis, I. Fuentes, and W. Dur, "Heisenberg scaling in Gaussian quantum metrology," *Phys. Rev. A* 92, 022106 (2015).
 29. C. M. Caves, "Quantum-mechanical noise in an interferometer," *Phys. Rev. D* 23, 1693 (1981).
 30. C. C. Gerry and P. L. Knight, *Introductory Quantum Optics*, 2nd ed. (Cambridge University Press, 2005).
 31. Y. Yamamoto and H. A. Haus, "Preparation, measurement and information capacity of optical quantum states," *Rev. Mod. Phys.* 58, 1001 (1986).
 32. P. Hello, in *Progress in Optics XXXVIII*, E. Wolf (editor). (Elsevier, 1998).
 33. The LIGO Scientific Collaboration, "Enhanced sensitivity of the LIGO gravitational wave detector by using squeezed states of light," *Nat. Photonics* 7, 613–619 (2013).
 34. M. Jarzyna and R. Demkowicz-Dobrzański, "Quantum interferometry with and without an external phase reference," *Phys. Rev. A* 85, 011801(R) (2012).
 35. J. D. Zhang, Z. J. Zhang, L. Z. Cen, J. Y. Hu, and Y. Zhao, "Nonlinear phase estimation: Parity measurement approaches the quantum Cramer-Rao bound for coherent states," *Phys. Rev. A* 99, 022106 (2019).
 36. S. Ataman, A. Preda, and R. Ionicioiu, "Phase sensitivity of a Mach-Zehnder interferometer with single-intensity and difference-intensity detection," *Phys. Rev. A* 98, 043856 (2018).
 37. A. Z. Goldberg, I. Gianani, M. Barbieri, F. Sciarrino, A. M. Steinberg, and N. Spagnolo, "Multiphase estimation without a reference mode," *Phys. Rev. A* 102, 022230 (2020).
 38. C. W. Helstrom, *Quantum Detection and Estimation Theory* (Academic Press, 1976).
 39. A. S. Holevo, *Probabilistic and Statistical Aspects of Quantum Theory* (Edizioni della Normale, 1982).
 40. S. L. Braunstein and C. M. Caves, "Statistical distance and the geometry of quantum states," *Phys. Rev. Lett.* 72, 3439 (1994).
 41. M. Takeoka, K. P. Seshadreesan, C. You, S. Izumi, and J. P. Dowling, "Fundamental precision limit of a Mach-Zehnder interferometric sensor when one of the inputs is the vacuum," *Phys. Rev. A* 96, 052118 (2017).
 42. C. Oh, S. Y. Lee, H. Nha, and H. Jeong, "Practical resources and measurements for lossy optical quantum metrology," *Phys. Rev. A* 96, 062304 (2017).
 43. P. M. Birchall, J. L. O'Brien, J. C. F. Matthews, and H. Cable, "Quantum-classical boundary for precision optical phase estimation," *Phys. Rev. A* 96, 062109 (2017).
 44. J. Liu, H. Yuan, X. M. Lu, and X. Wang, "Quantum Fisher information matrix and multiparameter estimation," *J. Phys. A: Math. Theor.* 53, 023001 (2020).
 45. V. V. Dodonov and V. I. Man'ko, *Theory of Nonclassical States of Light* (CRC Press, 2003).
 46. H. F. Hofmann, "All path-symmetric pure states achieve their maximal phase sensitivity in conventional two-path interferometry," *Phys. Rev. A* 79, 033822 (2009).
 47. W. L. You, Y. W. Li, and S. J. Gu, "Fidelity, dynamic structure factor, and susceptibility in critical phenomena," *Phys. Rev. E* 76, 022101 (2007).
 48. J. Liu, H. N. Xiong, F. Song, and X. Wang, "Fidelity susceptibility and quantum Fisher information for density operators with arbitrary ranks," *Physica A* 410, 167 (2014).
 49. P. M. Anisimov, G. M. Raterman, A. Chiruvelli, W. N. Plick, S. D. Huver, H. Lee, and J. P. Dowling, "Quantum metrology with two-mode squeezed vacuum: parity detection beats the Heisenberg limit," *Phys. Rev. Lett.* 104, 103602 (2010).